PROPAGATION OF CURVED FATIGUE CRACKS UNDER VARIABLE AMPLITUDE LOADING

Antonio Carlos de Oliveira Miranda, **Luiz Fernando Martha**
Pontifical Catholic University of Rio de Janeiro (PUC-Rio) - Dept. Civil Eng.
Rua Marquês de São Vicente, 225 Gávea, Rio de Janeiro, RJ 22453-900
amiranda@tecgraf.puc-rio.br, lfm@civ.puc-rio.br

Marco Antonio Meggiolaro, **Jaime Tupiassú Pinho de Castro**
Pontifical Catholic University of Rio de Janeiro (PUC-Rio) - Dept. Mechanical Eng.
Rua Marquês de São Vicente, 225 Gávea, Rio de Janeiro, RJ 22453-900
meggi@mec.puc-rio.br, jtcastro@mec.puc-rio.br

Abstract. *In this work, a two-step methodology to predict fatigue crack propagation in generic 2D structures is extended to variable amplitude loading histories, modeling crack retardation effects. Two complementary pieces of software have been developed to implement this methodology. In the first program, self-adaptive finite elements (FE) are used to calculate the fatigue crack path and the stress intensity factors along the crack length, at each propagation step. The computed values are then exported to the second program to predict the propagation fatigue life of the structure by the local approach, considering overload-induced crack retardation effects. To validate the methodology, fatigue crack growth experiments under variable amplitude (VA) loading are performed on 40mm-wide compact tension C(T) test specimens made of cold-rolled SAE 1020 steel, some of them modified with 7mm-diameter holes specially positioned to curve the crack path. FE predictions under constant amplitude (CA) loading indicated that depending on the hole position the crack could either curve its path and grow toward the hole ("sink in the hole" behavior) or just be deflected by the hole and continue to propagate after missing it ("miss the hole" behavior). Specimens presenting each of the behaviors are machined and tested under both CA and VA loadings, and the results are compared to crack growth predictions. The multiple overload effect on curved cracks is also studied, using 200mm-wide eccentrically-loaded single edge crack tension specimens ESE(T) made of SAE 4340 steel.*

Keywords*: fatigue, crack propagation, finite elements, variable amplitude, retardation models, multiple overloads*

1. Introduction

Fatigue life prediction under variable amplitude (VA) loading in intricate two-dimensional (2D) structural components requires the calculation of the generally curved crack path, the associated stress intensity factors (SIF), and the crack propagation rate at each load step. A finite element (FE) global discretization of the component - using an appropriate mesh with specialized crack tip elements - is a standard design practice to predict the crack path and to calculate its associated SIF $\mathbf{K_I}$ and $\mathbf{K_{II}}$. However, this global method is not computationally efficient under VA loading to predict fatigue lives, because it requires time-consuming remeshing procedures and FE recalculations of the entire structure stress/strain field after each event of the sequential rain-flow count of the loading. Moreover, if the modeling of crack retardation effects is required, the computational efficiency of this approach is, at least, severely compromised.

On the other hand, the local approach, based on the direct integration of the crack propagation equation, can be efficiently used to calculate the crack increment at each load cycle, considering crack retardation effects if necessary. However, this approach requires the stress intensity expression for the crack, which is not available for most real components. In these cases, the errors involved in using approximate $\mathbf{K_I}$ handbook expressions increase as the real crack deviates from the tabulated one, making the local approach accuracy questionable.

Since the advantages of the two approaches are complementary, the problem can be successfully divided into two steps (Miranda et al., 2002a). First, the (generally curved) fatigue crack path and its SIF are calculated under constant amplitude (CA) loading in a specialized FE program, using small crack increments and automatic mesh generation schemes. Numerical methods are used to calculate the crack propagation path, based on the computation of the crack incremental direction, and the SIF $\mathbf{K_I}$ and $\mathbf{K_{II}}$ generated by the FE program. Then, an analytical expression is fitted to the associated mode I SIF $\mathbf{K_I(a)}$, where **a** is the length along the crack path. This $\mathbf{K_I(a)}$ expression is used as an input to a general purpose fatigue design program based on the local approach, where the actual VA loading is efficiently treated by the integration of the crack propagation equation, considering overload-induced retardation effects if required.

This methodology has been experimentally validated through crack growth under CA loading experiments on modified compact tension C(T) specimens, in which holes were machined to curve the crack propagation path (Miranda et. al, 2002b). In this work, the methodology is extended to VA loading cases, considering load interaction effects.

2. Analytical Background

The two-step methodology described above requires specific methods to calculate the crack path and the associated SIF values, as well as the delay in crack growth caused by overloads. Three criteria can be used to obtain the crack path through the numerical computation of crack incremental growth direction in the linear-elastic regime: (i) the Maximum Circumferential Stress ($\boldsymbol{\sigma_{\theta max}}$), (ii) the Maximum Potential Energy Release Rate ($\mathbf{G_{\theta max}}$), and (iii) the Minimum Strain Energy Density ($\mathbf{U_{\theta min}}$) (Miranda, 2002a and 2002b). Then, to compute the SIF along the obtained path under mixed mode I - mode II loading, three methods are usually employed: (i) the displacement correlation technique (Shih, 1976),

(ii) the potential energy release rate computed by means of a modified crack-closure integral technique (Rybick, 1977; Raju, 1987), and (iii) the J-integral computed by means of the equivalent domain integral (EDI) together with a mode decomposition scheme (Dodds, 1988; Nikishkov, 1987). Bittencourt et al. (1996) showed that for sufficiently refined FE meshes all methods above predict essentially the same results.

The obtained crack path and SIF values are then used to calculate fatigue crack growth (FCG), considering load sequence interaction effects such as retardation induced by overloads (OL). Several retardation models have been developed based on OL-induced changes in the fatigue crack plastic envelope. These methods can be subdivided into three main categories (Schijve, 2001): (i) yield zone models, which account for retardation by comparing the OL and the current plastic zone sizes, $\mathbf{Z_{ol}}$ and $\mathbf{Z_i}$ (which could capture retardation caused by either crack closure or residual stress fields); (ii) crack closure models, which estimate the crack opening loads from experimental data; and (iii) strip-yield models, which numerically calculate the crack closure relations based on Dugdale's model (Koning et al, 1997).

Perhaps the best-known yield zone models are those developed by Wheeler (1972). The Wheeler model introduces a crack-growth reduction factor bounded by zero and unity. However, this model cannot predict OL-induced crack arrest. A simple but effective modification to the original Wheeler model can be used to predict both crack retardation and arrest in a continuous way. This approach, called the Modified Wheeler model (Meggiolaro & Castro, 2001), uses a Wheeler-like parameter to multiply **ΔK** instead of **da/dN** after the OL:

$$\Delta K_{ret}(a_i) = \Delta K(a_i) \cdot \left(\frac{Z_i}{Z_{ol} + a_{ol} - a_i} \right)^{\gamma}, \quad a_i + Z_i < a_{ol} + Z_{ol} \tag{1}$$

where $\mathbf{a_{ol}}$ and $\mathbf{a_i}$ are the crack sizes at the instant of the OL and at the (later) **i**-th cycle, $\mathbf{\Delta K_{ret}(a_i)}$ and $\mathbf{\Delta K(a_i)}$ are the values of the stress intensity ranges that would be acting at $\mathbf{a_i}$ with and without retardation due to the OL, and $\boldsymbol{\gamma}$ is an experimentally adjustable constant.

Among the crack closure models, probably the simplest is the Constant Closure model, originally developed at Northrop for use on their classified programs (Bunch, 1996). This load interaction model is based on the observation that for some load spectra the closure stresses do not deviate significantly from a certain stabilized value, which is assumed to be constant. The opening load $\mathbf{K_{op}}$ used in VA FCG calculations is generally estimated between 20% and 50% of the maximum OL.

Another crack closure model is Newman's (Newman, 1984), who concluded from FE calculations that crack closure depends not only on the load ratio **R**, but also on the ratio between the maximum stress level $\boldsymbol{\sigma_{max}}$ and the material flow strength $\mathbf{S_{fl}}$, and on a stress-state (plane stress / plane strain) constraint factor $\boldsymbol{\alpha}$. This stress-state constraint typically ranges from $\boldsymbol{\alpha = 1}$ for pure plane-stress (but a value $\boldsymbol{\alpha = 1.15}$ has a better agreement with experimental results) to $\boldsymbol{\alpha = 1/(1 - 2\nu)}$ for pure plane-strain, where $\boldsymbol{\nu}$ is Poisson's ratio.

As discussed above, one OL cycle can result in a considerable delay of FCG. However, it has been observed that a greater number of consecutive OL cycles can result in larger retardation, a phenomenon called the *multiple OL effect*. Dahl and Roth (1979) performed tests on 1020 steel, observing a larger delay period after multiple OL-cycles, see Fig. (1). They found out that the number of delay cycles $\mathbf{n_D}$ systematically increased with the number of consecutive applied overloads $\mathbf{n_{OL}}$. As seen in Fig. (1), at least 600 consecutive OL were necessary to achieve the maximum retardation in these tested specimens.

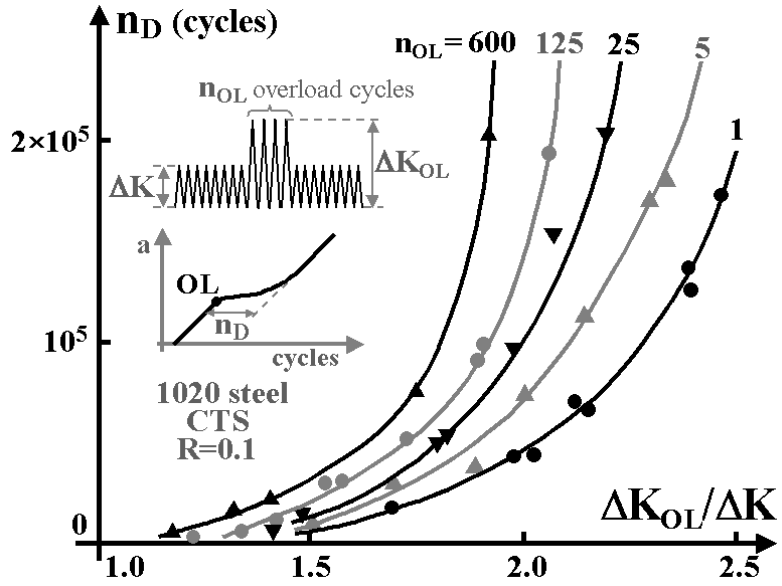

Figure 1. Influence of the number of OL cycles $\mathbf{n_{OL}}$ and the overload ratio $\mathbf{\Delta K_{OL}/\Delta K}$ on the crack growth delay period $\mathbf{n_D}$ (adapted from Dahl & Roth, 1979).

A reasonable explanation for such effect is based on Elber's closure mechanism: since crack extension occurs during the OL, more OL cycles will leave a longer wake of plastic deformation behind the crack tip (with length initially equal to the crack growth during the multiple OL cycles), increasing crack closure and retardation levels. In this case, delayed retardation may not be observed because immediately after the multiple OL block an inflated plastic wake will already be present. Therefore, retardation will be observed even before the crack tip cuts through the plastic zone generated by the last OL of the block. However, the retardation models discussed above do not explicitly account for the *multiple OL effect*. This issue is addressed in section 4.2.

Two complementary pieces of software, named **Quebra2D** and **ViDa** (Miranda, 2002a and 2002b; Meggiolaro & Castro, 1998), have been developed to implement the described two-step hybrid methodology. A brief description of both programs is presented in the next section.

3. Crack Propagation Software

Quebra2D is an interactive graphical program for simulating two-dimensional fracture processes based on a finite-element self-adaptive mesh-generation strategy (Miranda, 2002b; Wawrzynek, 1987). This program includes all methods described above to compute the crack increment direction and the associated stress-intensity factors along the crack path. The crack representation scheme used in the **Quebra2D** program is based on the discrete approach, similar to well-known 2D simulators such as **Franc2D** (Wawrzynek, 1987). However, **Quebra2D** brings some improvements with respect to its predecessors. It performs adaptive FE analyses, and its graphical interfaces are much more flexible and portable. Moreover, the adaptive FE analyses are coupled with modern and very efficient automatic remeshing schemes, which substantially decrease the required computational time.

The automatic calculation procedure in **Quebra2D** is performed in 4 steps: (i) the FE model of the cracked structure is solved to obtain $\mathbf{K_I}$ and $\mathbf{K_{II}}$ and to calculate the corresponding crack propagation direction; (ii) the crack is increased in the growth direction by a (small) required step; (iii) the model is remeshed to account for the new crack size; and (iv) the process is iterated until rupture or until a specified crack size is reached. As a result, a list of $\mathbf{K_I}$ and $\mathbf{K_{II}}$ values is generated at short but discrete intervals along the predicted crack paths.

The second program, named **ViDa**, is a general-purpose fatigue design program developed to predict both initiation and **propagation** fatigue lives under VA loading by all classical design methods, including the **SN**, the **IIW** (for welded structures) and the **εN** for crack initiation, and the **da/dN** for crack propagation (ViDa, htpp). It includes several load interaction models, predicting overload and underload-induced crack retardation and acceleration. This program does not require the global solution of the structure's stress field because it is based on the local approach, since its crack growth module is based on the direct integration of the fatigue crack propagation equation of the material, $\mathbf{da/dN = F(\Delta K, R, \Delta K_{th}, K_C, ...)}$, where $\mathbf{\Delta K}$ is the stress intensity range, $\mathbf{R = K_{min}/K_{max}}$ is the load ratio, $\mathbf{\Delta K_{th}}$ is the fatigue crack propagation threshold, and $\mathbf{K_C}$ is the fracture toughness of the structure. The program includes comprehensive database with hundreds of editable $\mathbf{K_I}$ and $\mathbf{K_{II}}$ SIF expressions and **da/dN** curves to be used in the calculations. In particular, **ViDa** accepts any crack growth equation and any SIF expression, making it an ideal companion to **Quebra2D**, which can be used to generate the required **ΔK** expression if not available in its database.

4. Experimental Results

4.1. Experiments on modified compact tension specimens

FCG experiments were performed on compact tension C(T) test specimens, some of them modified with holes specially positioned to curve the crack path. The specimens were made of cold-rolled SAE 1020 steel with yield strength **285MPa**, ultimate strength **491MPa**, Young modulus **205GPa**, and reduction in area **54%**, measured according to the ASTM E 8M-99 standard, with the analyzed weight percent composition shown in Table (1). The FCG tests were performed at two **R** ratios, **R = 0.1** and **R = 0.7**, in a 250kN computer-controlled servo-hydraulic testing machine. The crack length was measured following ASTM E 647-99 procedures. The measured growth rates on 16 standard C(T) specimens were fitted by a modified McEvily **da/dN** equation (in m/cycle), as shown in Fig. (2), where $\mathbf{\Delta K_0 = 11.5\ MPa\sqrt{m}}$ is the propagation threshold under **R = 0**, and the fracture toughness is $\mathbf{K_C = 280\ MPa\sqrt{m}}$.

Table 1 - Chemical composition of the tested SAE 1020 steel (weight %)

C	Mn	Si	Ni	Cr	Mo	Cu	Nb	Ti	S	P	Fe
0.19	0.46	0.14	0.052	0.045	0.007	0.11	0.002	0.002	0.04	0.035	balance

Three modified C(T) specimens have been designed and tested, with w = 29.5 mm and t = 8 mm. Each one had a 7mm-diameter hole positioned at a slightly different horizontal distance **A** and vertical distance **B** from the notch root, as shown in Fig. 3. This odd configuration was chosen because two very different crack growth behaviors had been predicted by the FE modeling of the holed C(T) specimens, depending on the hole position. The predictions indicated that the fatigue crack was always attracted by the hole, but it could either curve its path and grow toward the hole ("sink in the hole" behavior) or just be deflected by the hole and continue to propagate after missing it ("miss the hole" behavior).

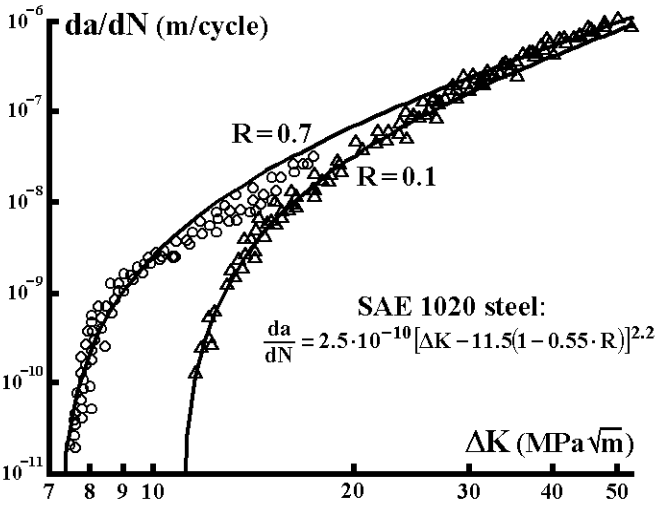

Figure 2. Modified McEvily da/dN equation fitted to the SAE 1020 steel data.

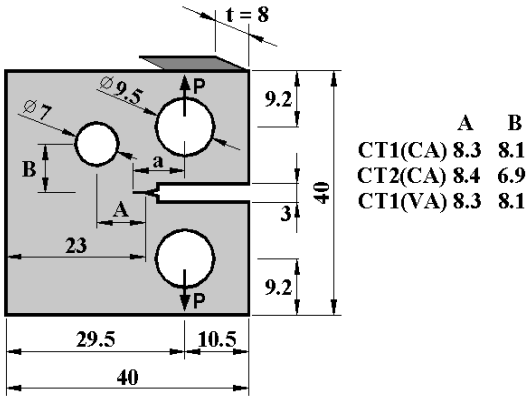

Figure 3. Measured dimensions of the hole-modified C(T) specimens (mm).

Using the **Quebra2D** program, the transition point between the "sink in the hole" and the "miss the hole" crack growth behaviors was identified. The three modified C(T) specimens were designed so that specimens named CT1(CA) and CT1(VA) had the hole just half a millimeter above the transition point, and a specimen named CT2(CA) had the hole half a millimeter below it. The chosen specimen geometries were machined, measured, and FE remodeled, to account for small deviations in the machining process, see Fig. (4). In this way, it could be assured that the numerical models used in the predictions reproduced the real geometry of the tested specimens.

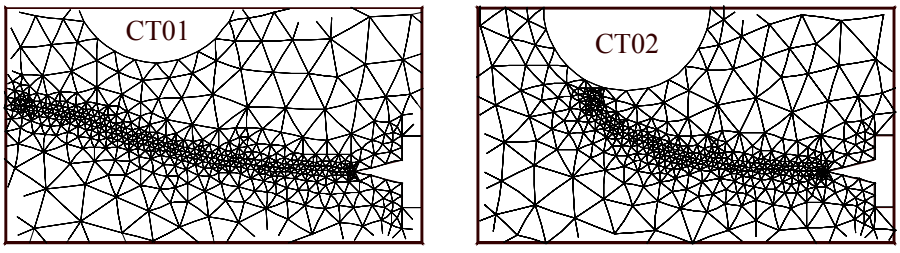

Figure 4. FE mesh automatically generated for the modified specimens CT1(CA) and CT2(CA).

Specimens CT1(CA) and CT2(CA) were tested under CA loading, with a quasi-constant stress-intensity range around $\Delta K_I \approx 20 MPa\sqrt{m}$ and load ratio **R = 0.1**. These loading values induce a stage-II (Paris regime) crack growth in the 1020 steel.

Two specimens were tested under VA loading: one standard C(T) specimen, and the holed specimen CT1(VA). The goals of this experiment were: (i) to check whether the curved crack paths predicted under CA loading would give good estimates of the measured paths under VA loading; (ii) to verify whether load interaction models calibrated for straight cracks in the standard C(T) could be used to predict the fatigue life of the holed specimens, which present a curved crack path. The VA load histories applied to the specimens are shown in Fig. (5).

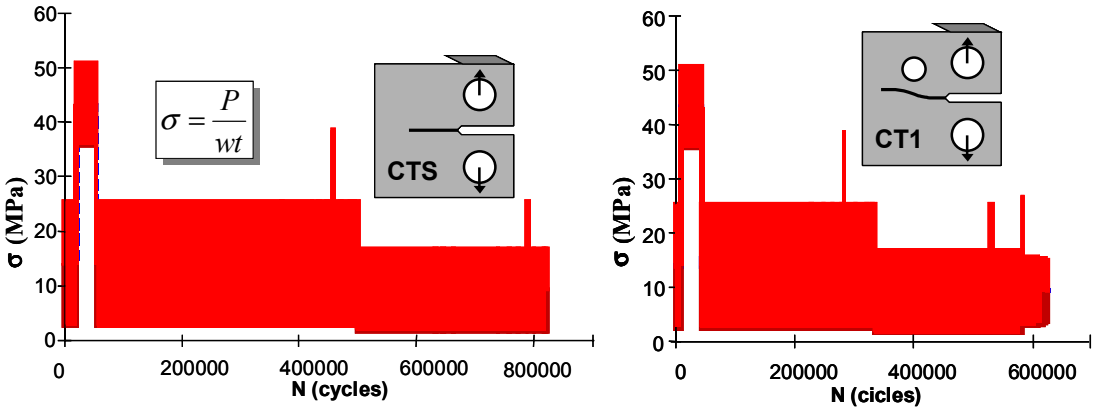

Figure 5. Applied load history for standard C(T) and modified CT1(VA) specimens.

Figure (6) shows the predicted and measured crack paths for the three modified specimens (in mm) under CA or VA loading, presenting a very good match. This suggests that the crack path under VA loading is the same as the one predicted under CA loading, under Linear Elastic Fracture Mechanics. Therefore, assuming that only the crack growth rate (but not its path) is influenced by load interaction effects, the discussed two-step methodology can be generalized to the VA loading case.

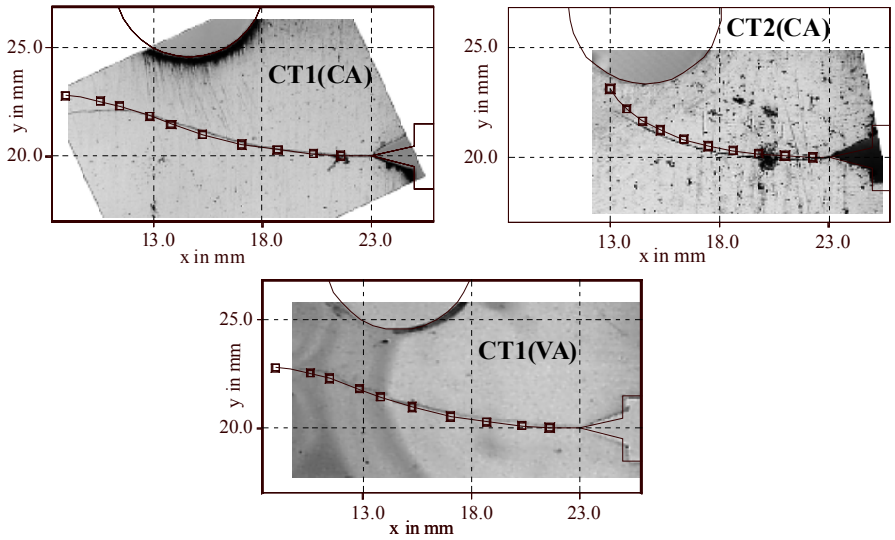

Figure 6. Predicted and measured crack paths for the three modified C(T) specimens (mm).

The SIF values calculated under CA loading along the crack path using the **Quebra2D** program were exported to the **ViDa** software to predict fatigue life, considering load interaction effects if necessary. Figure (7) shows a very good match between predicted and measured crack sizes for the modified C(T) specimens under CA loading. The curved-crack predictions were based solely on crack growth data measured for straight-cracks and on SIF expressions calculated for the hole-modified specimens using FE.

To evaluate whether load interaction models calibrated from straight-crack experiments can be applied to specimens with curved cracks, several crack retardation models were calibrated (fitted) based on the standard C(T) data under VA loading. Several models were considered, and the better results were obtained by the Constant Closure model, where $\mathbf{K_{op}}$ was calibrated as 26% of the maximum overload SIF, $\mathbf{K_{ol,max}}$; by the Modified Wheeler model, where the exponent $\boldsymbol{\gamma}$ was estimated as 0.51; and by Newman's closure model (generalized for the VA loading case), where the stress-state constraint was fitted as $\boldsymbol{\alpha = 1.07}$, a value suggesting dominant plane-stress FCG conditions. The measured and fitted growth behavior is shown in Fig. (8).

The fitted load interaction parameters were then used to predict the crack growth behavior under VA loading of the hole-modified CT1(VA) specimen, see Fig. (9). The significant retardation effects of the CT1(VA) specimen were very well predicted using these three load interaction models in the **ViDa** program. In particular, the Modified Wheeler model results in very good predictions, possibly because its simplistic empirical yield-zone formulation can account for both closure and residual stress effects. These results suggest that load interaction models calibrated using straight cracks can be used to predict crack retardation behavior of curved cracks under VA loading.

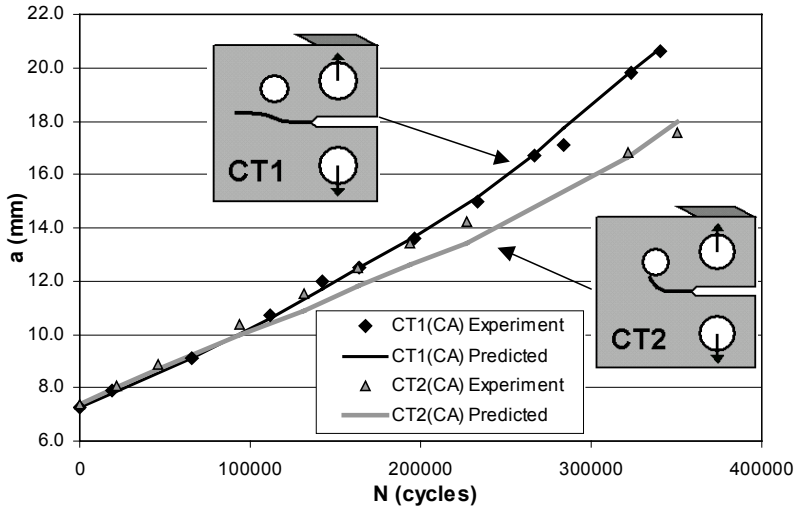

Figure. 7. Predicted and measured fatigue crack growth for modified C(T) specimens under CA loading.

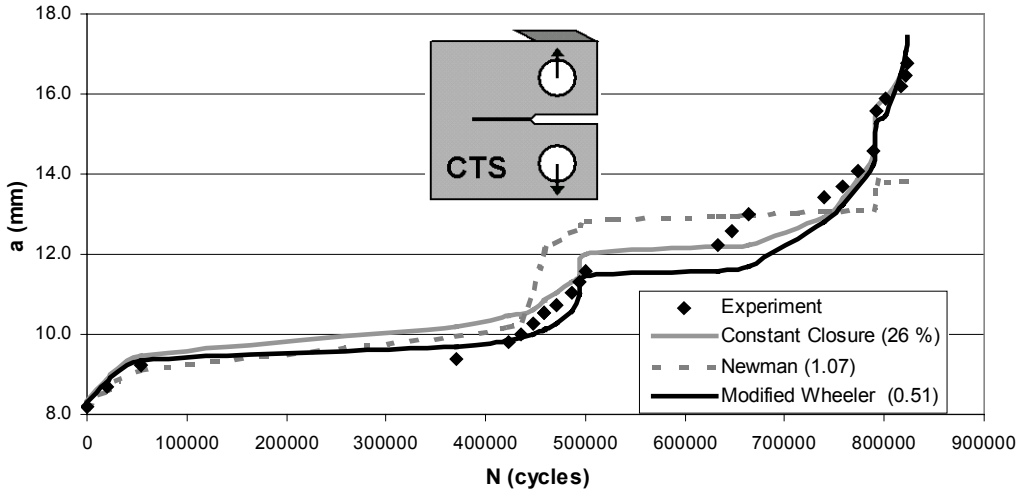

Figure 8. Measured crack sizes and calibrated calculations on a standard C(T) under VA loading.

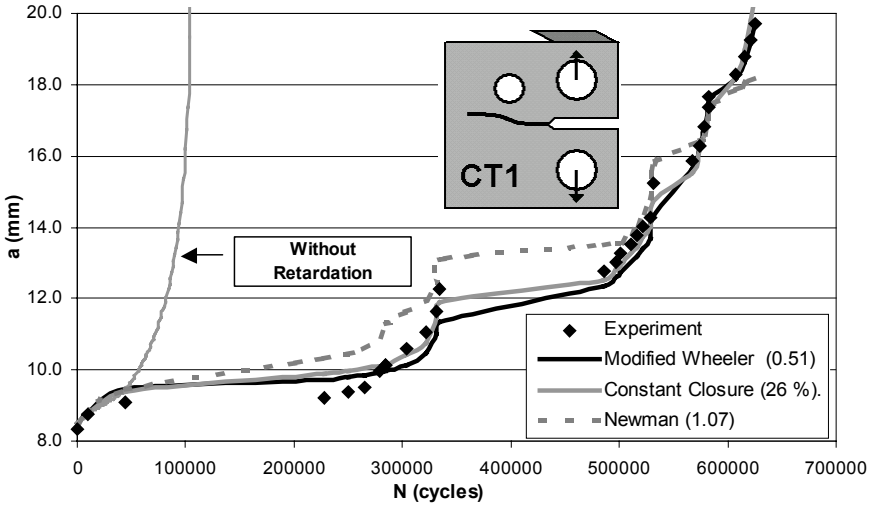

Figure 9. Crack growth predictions (based on straight-crack calibrations) on a modified C(T) specimen under VA loading.

However, it must be pointed out that the VA histories in Fig. (5) are very similar in nature, with similar stress levels and overload ratios. This similarity might be one of the reasons why the same load interaction model parameters could be used for both VA cases. The load-spectrum dependency of the crack retardation model parameters might result in poor predictions if completely different VA histories are considered.

4.2. Experiments on eccentrically-loaded single edge crack tension specimens

FCG experiments were performed on Eccentrically-Loaded Single Edge Crack Tension Specimens ESE(T), with dimensions shown in Fig. (10). The specimens were made of cold-rolled SAE 4340 steel with yield strength **377MPa**, ultimate strength **660MPa**, Young modulus **205GPa**, and reduction in area **52.7%**, measured according to the ASTM E 8M-99 standard, with the analyzed weight percent composition shown in Table (2).

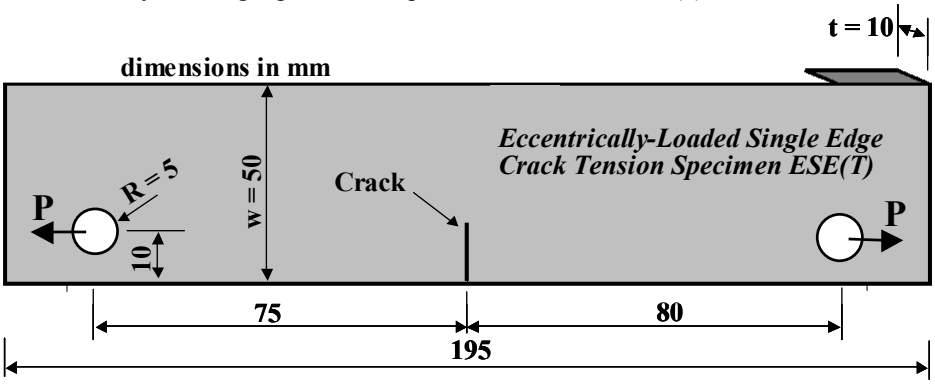

Figure 10. Measured dimensions of the ESE(T) specimens (mm).

Table 2 - Chemical composition of the tested SAE 4340 steel (weight %)

C	Mn	Si	Ni	Cr	S	P	Mo	Fe
0.37	0.56	0.14	1.53	0.64	0.04	0.035	0.18	balance

The tests were performed at two **R** ratios, **R = 0.1** and **R = 0.7**, in a 250kN computer-controlled servo-hydraulic testing machine. The crack length was measured following ASTM E 647-99 procedures. The measured growth rates were fitted by a modified Collipriest **da/dN** equation (in m/cycle)

$$\frac{da}{dN} = 2.4 \cdot 10^{-10} \left[K_C \cdot \Delta K_0 \cdot FR \cdot \left(\frac{K_C}{\Delta K_0 \cdot FR} \right)^{0.5 \cdot \ln \left(\frac{\ln\left(\frac{\Delta K}{\Delta K_0 \cdot FR} \right)}{\ln\left(\frac{K_C}{\Delta K} \right)} \right)} \right]^{1.25} \tag{2}$$

where **FR = (1 – 1.1·R)**, the propagation threshold under **R = 0** is ΔK_0 **= 8.5 MPa√m**, and K_C **= 300 MPa√m** is the fracture toughness. The measured FCG curves of the SAE 4340 steel at these two **R** ratios are shown in Fig. (11).

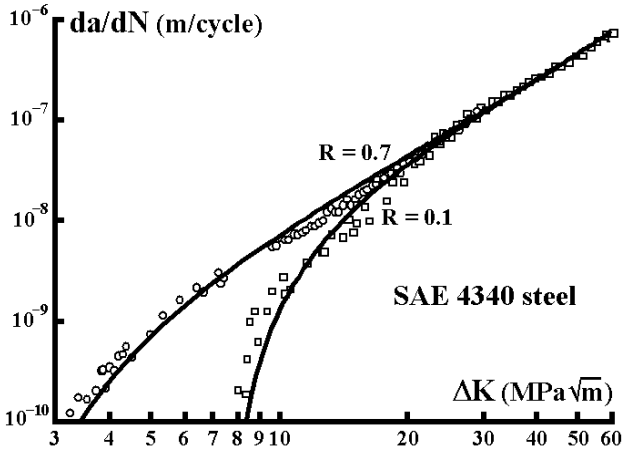

Figure 11. Modified Collipriest da/dN equation fitted to the SAE 4340 steel data.

The ESE(T) specimens were tested under the load history shown in Fig. (12). This VA history is divided into six load blocks of two different types. Blocks 1, 2 and 3 are *single-OL blocks*, because they consist basically of CA cycles during which single overloads are applied. Blocks 4, 5 and 6 are *multiple-OL blocks*, because they start with a large reduction in load level followed by CA cycles, which can be regarded as baseline events following multiple overloads. Therefore, a relatively larger retardation effect is expected in blocks 4, 5 and 6 due to the *multiple OL effect* (section 2).

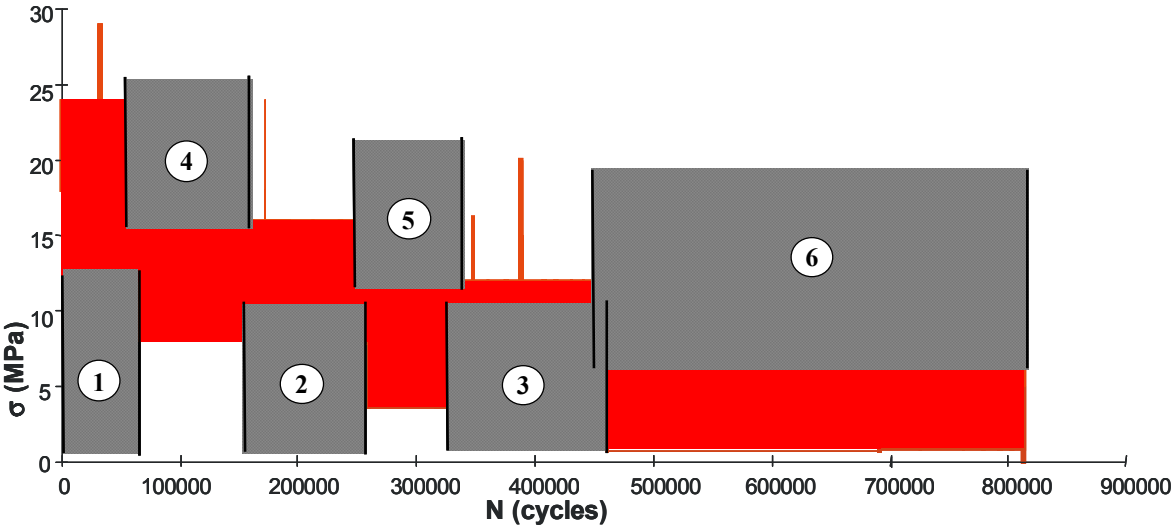

Figure 12. Load history applied to the ESE(T) specimens (in red) and subdivision into six load blocks (in gray).

Three crack retardation models were calibrated to the experimental FCG data: Constant Closure, Modified Wheeler, and Newman's closure model generalized for the VA loading case. The predictions based on the calibrated parameters fitted very poorly the experimental data, because the applied models do not consider explicitly the influence of the number of OL cycles.

On the other hand, if different retardation parameters are fitted to the single-OL and to the multiple-OL blocks, then reasonably accurate predictions can be obtained. Table (3) shows the obtained retardation parameters for each block type, including Constant Closure's ratio between $\mathbf{K_{op}}$ and $\mathbf{K_{ol,max}}$, Modified Wheeler's exponent $\boldsymbol{\gamma}$, and Newman's stress-state parameter $\boldsymbol{\alpha}$. The crack growth predictions are shown in Figures (13-15), where the black and gray lines are obtained respectively from the retardation parameters for the single and multiple-OL blocks.

Table 3 – Retardation parameters fitted to single and multiple-OL blocks

	single-OL blocks	multiple-OL blocks
Constant Closure $\mathbf{K_{OP}/K_{ol,max}}$	0.22	0.37
Modified Wheeler $\boldsymbol{\gamma}$	0.11	0.80
Newman $\boldsymbol{\alpha}$	3.0	1.7

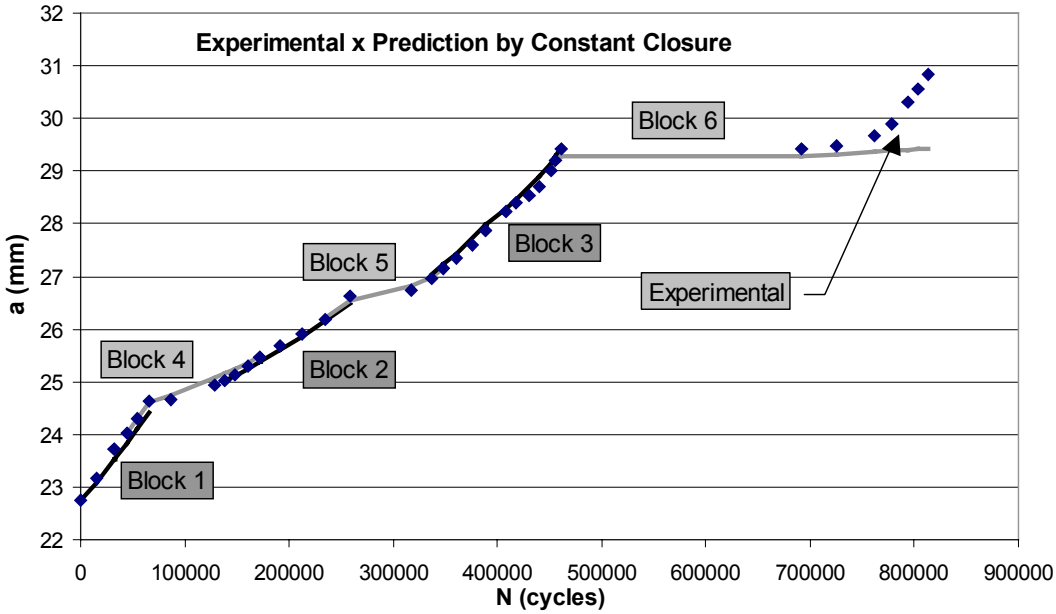

Figure 13. FCG predictions for each load block using the Constant Closure model.

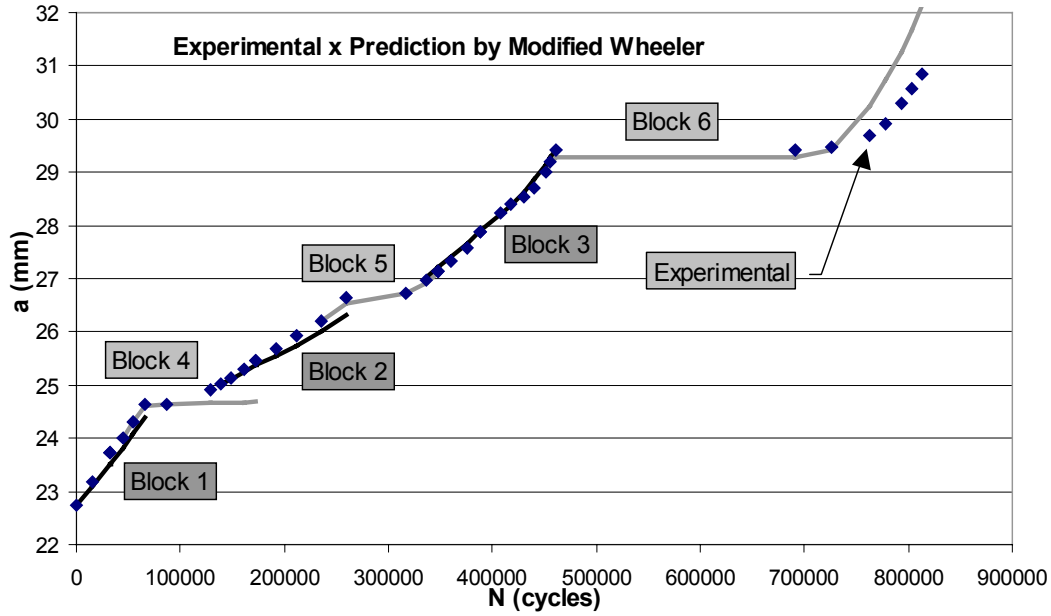

Figure 14. FCG predictions for each load block using the Modified Wheeler model.

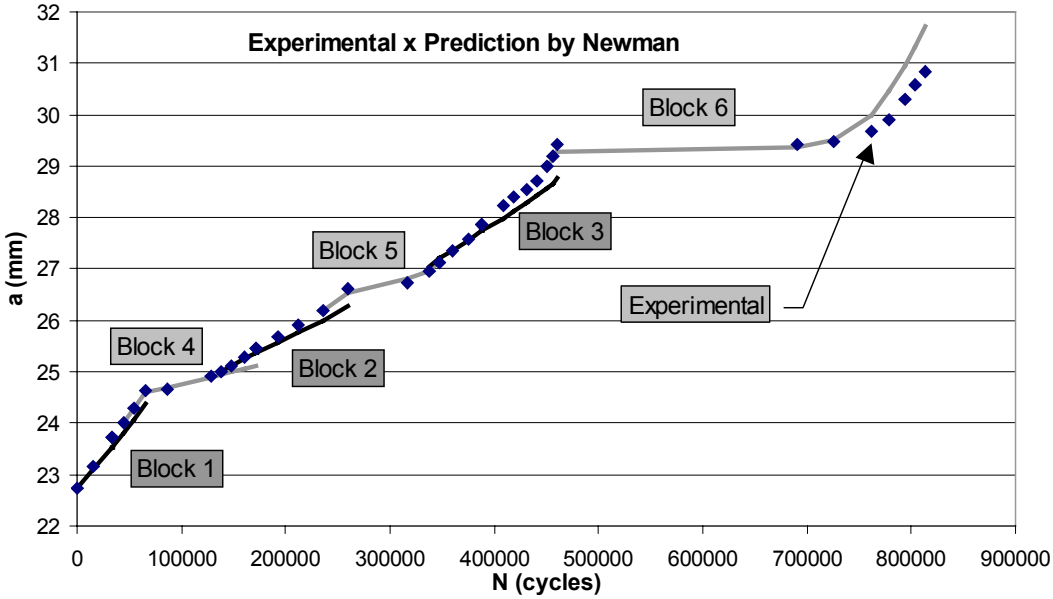

Figure 15. FCG predictions for each load block using Newman's closure model.

As seen in Table (3), in this experiment the fitted Constant Closure model parameters result in an opening SIF equal to 22% of the maximum overload level of the single-OL blocks. However, for the multiple-OL blocks this percentage rises to 37%, increasing crack closure and therefore retardation effects. Similarly, increased retardation is found in the presence of multiple overloads as the Modified Wheeler exponent rises from 0.11 to 0.80.

Finally, Newman's stress-state parameter α is calibrated as 3.0 for single-OL blocks, suggesting a dominant plane-strain condition. But for the multiple-OL blocks the parameter α is artificially lowered to 1.7. This lower value is associated with stress-state conditions closer to plane-stress, where larger OL plastic zones result in increased closure and retardation levels, confirming the significance of the multiple-OL effect.

6. Conclusions

In this paper, a methodology to predict fatigue crack propagation in generic 2D structures was extended to variable amplitude loading histories. Fatigue crack growth experiments under variable amplitude (VA) loading were performed on compact tension C(T) test specimens made of cold-rolled SAE 1020 steel, some of them modified with 7mm-diameter holes specially positioned to curve the crack path. It was found that the measured crack paths under VA loading were well estimated by the curved paths predicted using FE under CA loading, suggesting that overloads do not significantly deviate the crack growth direction. In addition, load interaction models calibrated for straight cracks in

standard C(T) specimens were successfully used to predict the fatigue life of the holed specimens under variable amplitude loading. The multiple overload effect on curved cracks was also studied on eccentrically-loaded single edge crack tension specimens ESE(T) made of SAE 4340 steel. Using different crack retardation parameters for single and multiple overloads, it was possible to obtain reasonably accurate crack growth predictions. The load interaction parameters calibrated after multiple overloads were associated with much larger retardation effects than those calibrated after single overloads, confirming Dahl and Roth's observations. Therefore, the experimental results validated the application of the proposed methodology to the variable amplitude loading case.

7. References

Bittencourt, T.N., Wawrzynek, P.A., Ingraffea, A.R., Sousa, J.L.A., 1996, "Quasi-Automatic Simulation of Crack Propagation for 2D LEFM Problems," Eng. Fracture Mechanics; 55:321-334.

Bunch, J.O., Trammell, R.T., Tanouye, P.A., 1996, "Structural Life Analysis Methods used on the B-2 Bomber," Advances in Fatigue Lifetime Predictive Techniques: 3rd Volume, A96-26758 06-39, ASTM:220-247.

Dahl, W., Roth, G., 1979, "On the Influence of Overloads on Fatigue Crack Propagation in Structural Steels," Aachen Technical University.

Dodds, R.H. Jr, Vargas, P.M., 1988, "Numerical Evaluation of Domain and Contour Integrals for Nonlinear Fracture Mechanics," Dept. of Civil Eng., U. of Illinois, Urbana-Champaign.

de Koning, A.U., ten Hoeve, H.J., Hendriksen, T.K., 1997, "The Description of Crack Growth on the Basis of the Strip-Yield Model for Computation of Crack Opening Loads, the Crack Tip Stretch and Strain Rates," National Aerospace Lab. (NLR), Report NLR-TP-97511L.

Meggiolaro, M.A., Castro, J.T.P., 1998, "ViDa - a Visual Damagemeter to Automate the Fatigue Design under Complex Loading" (in Portuguese), Journal of the Brazilian Society of Mechanical Sciences; 20:666-685.

Meggiolaro, M.A., Castro, J.T.P., 2001, "An Evaluation of Elber-Type Crack Retardation Models," II SAE-Brazil International Fatigue Seminar, SAE #2001-01-4063, SAE 2001:207-216.

Meggiolaro, M.A., Castro, J.T.P., Miranda, A.C.O., Martha, L.F., Bittencourt, T.N., 2001, "Prediction of Fatigue Life and Crack Path in Generic 2D Structural Components under Complex Loading", *16th International Congress of Mechanical Engineering (COBEM)*, ABCM, Uberlândia, MG; 12:257-266

Miranda, A.C.O., Meggiolaro, M.A., Castro, J.T.P., Martha, L.F., Bittencourt, T.N., 2002a, "Fatigue Crack Propagation under Complex Loading in Arbitrary 2D Geometries," In: Braun AA, McKeighan PC, Lohr RD, eds. Applications of Automation Technology in Fatigue and Fracture Testing and Analysis, ASTM STP 1411(4):120-145.

Miranda, A.C.O., Meggiolaro, M.A., Castro, J.T.P., Martha, L.F., Bittencourt, T.N., 2002b, "Fatigue Life and Crack Path Prediction in Generic 2D Structural Components," Engineering Fracture Mechanics, 70:1259-1279.

Newman, J.C. Jr. ,1984, "A Crack Opening Stress Equation for Fatigue Crack Growth," Int Journal of Fracture; 24(3):R131-R135.

Nikishkov, G.P., Atluri, S.N., 1987, "Calculation of Fracture Mechanics Parameters for an Arbitrary Three-Dimensional Crack by the Equivalent Domain Integral Method," Int. J. for Numerical Methods in Eng.; 24:1801-1821.

Raju, I.S., 1987, "Calculation of Strain-Energy Release Rates with Higher Order and Singular Finite Elements," Engineering Fracture Mechanics; 28:251-274.

Rybicki, E.F., Kanninen, M.F., 1977, "A Finite Element Calculation of Stress-Intensity Factors by a Modified Crack Closure Integral," Engineering Fracture Mechanics; 9:931-938.

Schijve, J., 2001, "Fatigue of Structures and Materials," Kluwer Academic Publishers.

Shih, C.F., de Lorenzi, H.G., German, M.D., 1976, "Crack Extension Modeling with Singular Quadratic Isoparametric Elements," International Journal of Fracture; 12:647-651.

ViDa, homepage http://www.tecgraf.puc-rio.br/vida

Wawrzynek, P.A., Ingraffea, A.R., 1987, "Interactive Finite Element Analysis of Fracture Processes: An Integrated Approach," Theoretical and Applied Fracture Mechanics; 8:137-150.

Wheeler, O.E., 1972, "Spectrum Loading and Crack Growth," J of Basic Engineering: 181-186.